

GENERAL INSTRUCTION

- **Authors:** Carefully check the page proofs (and coordinate with all authors); additional changes or updates WILL NOT be accepted after the article is published online/print in its final form. Please check author names and affiliations, funding, as well as the overall article for any errors prior to sending in your author proof corrections. Your article has been peer reviewed, accepted as final, and sent in to IEEE. No text changes have been made to the main part of the article as dictated by the editorial level of service for your publication.
- **Authors:** We cannot accept new source files as corrections for your article. If possible, please annotate the PDF proof we have sent you with your corrections and upload it via the Author Gateway. Alternatively, you may send us your corrections in list format. You may also upload revised graphics via the Author Gateway.

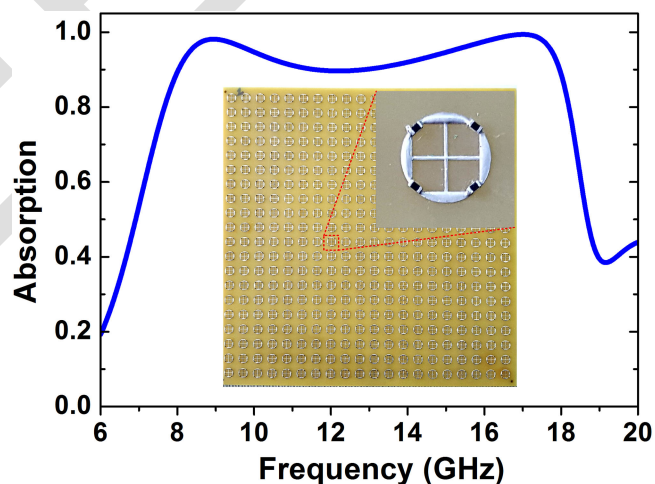
Queries

- Q1. Author: Please provide the postal code in the affiliation of authors Thi Kim Thu Nguyen, Thanh Nghia Cao, Ngoc Hieu Nguyen, Le Dac Tuyen, Xuan Khuyen Bui, Chi Lam Truong, Dinh Lam Vu, and Thi Quynh Hoa.Nguyen.
- Q2. Author: Please confirm or add details for any funding or financial support for the research of this article.
- Q3. Author: Please provide full page range in Refs. [2], [4], [7], [8], [27], [39], [41], [52], [59].

Simple Design of a Wideband and Wide-Angle Insensitive Metamaterial Absorber Using Lumped Resistors for X- and Ku-Bands

Volume 13, Number 3, June 2021

Thi Kim Thu Nguyen
Thanh Nghia Cao
Ngoc Hieu Nguyen
Le Dac Tuyen
Xuan Khuyen Bui
Chi Lam Truong
Dinh Lam Vu
Thi Quynh Hoa Nguyen



DOI: 10.1109/JPHOT.2021.3085320

Simple Design of a Wideband and Wide-Angle Insensitive Metamaterial Absorber Using Lumped Resistors for X- and Ku-Bands

Thi Kim Thu Nguyen,^{1,2} Thanh Nghia Cao,¹ Ngoc Hieu Nguyen,¹
Le Duc Tuyen,³ Xuan Khuyen Bui,⁴ Chi Lam Truong,⁵ Dinh Lam Vu,²
and Thi Quynh Hoa Nguyen ¹

Q1

¹ School of Engineering and Technology, Vinh University, Vinh, Vietnam
² Graduate University of Science and Technology, Vietnam Academy of Science and Technology, Hanoi, Vietnam
³ Department of Physics, Hanoi University of Mining and Geology Hanoi, Vietnam
⁴ Institute of Materials Science, Vietnam Academy of Science and Technology, Hanoi, Vietnam
⁵ NTT Hi-Tech Institute, Nguyen Tat Thanh University, Ho Chi Minh City, Vietnam

DOI:10.1109/JPHOT.2021.3085320

This work is licensed under a Creative Commons Attribution 4.0 License. For more information, see <https://creativecommons.org/licenses/by/4.0/>

Q2

Manuscript received March 8, 2021; revised May 26, 2021; accepted May 26, 2021. This work was supported in part by the Ministry of Education and Training, Vietnam under Grant B2021-TDV-05. Corresponding author: Thi Quynh Hoa Nguyen (e-mail: ntqhoa@vinhuni.edu.vn).

Abstract: We report a wideband and polarization-/wide-angle insensitive metamaterial absorber based on a symmetry structure associated with surface mount resistors. The proposed structure consists of a periodic array of a top metal symmetry resonator loading with four lumped resistors and a continuous metal ground plane separated by a dielectric substrate of FR-4. A prototype of the proposed absorber is fabricated and measured, confirming a good agreement between the measurement and simulation results. The proposed absorber shows polarization-insensitive behavior and the absorption response in a frequency range from 8-18 GHz covering the entire X- and Ku- bands with an absorptivity above 80% for a wide incident angle up to 40° for both transverse electric and transverse magnetic polarizations. Compared with the reported broadband absorbers using lumped resistors, our proposed absorber exhibits excellent characteristics in terms of compact and simple structure, high relative absorption bandwidth, and polarization and wide-incident insensitivity. Therefore, this design shows promising potential for both X- and Ku-band applications.

Index Terms: Holography, image analysis.

I. Introduction

Metamaterials have attracted enormous attention with various potential applications in perfect lens [1]–[3], holograms [4], [5], invisibility cloaking [6], [7], polarization converter [8], [9] and perfect absorber [10], [11] due to their exotic properties. Among them, metamaterial absorber (MA) is one of the fastest-growing field for solar cells [12], [13], thermal emitter [14]–[16], antenna design [17], [18], and imaging and sensing [11], [19]–[21] applications. Until now, the MAs have been realized to absorb the EM waves from microwave, infrared to visible region. However, the bandwidth of MA

45 is narrow because of its natural resonance. Therefore, many approaches have been proposed to
46 extend the bandwidth of MAs such as using planar arrangement of various sizes of resonators in
47 unit-cell [22]–[25], vertical stacking of metal-dielectric multilayer [26]–[30], and planar fractal struc-
48 ture [31]–[34]. Despite broadening of absorption bandwidth, some problems have been made by
49 these methods. For example, the fabrication process of vertical stacking is very complicated, while
50 the planar arrangement method possesses functional limitations such as polarization-dependency
51 and sensitivity to oblique incidence [35]. Meanwhile, the design of broadband MA based on a
52 planar fractal structure is not efficient in microwave range [34]. Recently, the symmetry structures
53 based on lumped elements can be considered as an emerging and promising alternative for
54 designing the broadband absorber with large enough bandwidth, high efficiency, and polarization
55 insensitivity [36]–[42]. Li *et al.* proposed the thin and polarization-insensitive wideband MA formed
56 by loading eight lumped resistors into double octagonal rings, which showed a 9.25 GHz-wide
57 absorption from 7.93 to 17.18 GHz with absorptivity larger than 90%, however, the angular stability
58 is still small below 20°[36]. Chen *et al.* designed a microwave metamaterial absorber using lumped
59 resistors and metallic via holes which exhibited the absorption bandwidth covering the entire
60 X- and Ku-bands [41]. Furthermore, Bagmanci *et al.* demonstrated the polarization-independent
61 broadband MA structure created by loaded with the lumped resistors and via connection lines
62 into split-ring resonators. The simulation results indicate that the proposed broadband absorber
63 achieved a perfect absorption from 4 GHz to 16 GHz [42]. The combination of metallic shorting
64 pins and lumped resistors can be good candidates for broadening the absorption bandwidth and
65 keeping the wide angular stability [41], [42], but this method still needs a complex manufacturing
66 process, thus resisting their practical applications. Therefore, the design of the MA based on
67 lumped resistors is facing significant challenges to achieve a simple structure, wide bandwidth,
68 and good absorption performance such as polarization and wide incident angle insensitivity,
69 simultaneously.

70 Herein, we propose a simple design of an ultra-broadband and wide-angle and polarization
71 insensitive MA using symmetry structure loading by lumped resistors operating in X- and Ku-
72 bands. The proposed MA is composed of a periodic array of a metal symmetry-shaped resonator
73 loaded by four lumped resistors, and a dielectric substrate of FR4 backed with a bottom metal
74 continuous ground plane. The absorption performance of the proposed MA is numerically and
75 experimentally investigated. The designed MA achieves an ultra-broadband absorption response
76 with the absorptivity above 90% in the frequency range from 8 to 18 GHz covering the entire X- and
77 Ku-bands. Moreover, the absorption efficiency is retained higher than 80% in the whole band with
78 a wide incident angle for both transverse electric (TE) and transverse magnetic (TM) polarizations.
79 Therefore, this designed structure can be used for X- and Ku-band applications.

80 II. Structure Design and Method

81 Fig. 1 shows a schematic of the proposed MA. The unit cell of the proposed MA consists of a
82 metallic resonator loaded with four lumped resistors and a dielectric substrate backed by a metal
83 continuous ground plane, as presented in Fig. 1(a). The dielectric substrate is made by FR-4 with
84 the thickness (h) of 2.5 mm. The FR-4 substrate has a relative dielectric constant of 4.3 and a loss
85 tangent of 0.025. The top and the bottom layers are made of copper with an electric conductivity of
86 5.96×10^7 S/m and a thickness of 0.035 mm. This study aims to design a broadband MA operating
87 in the range of 8–18 GHz, which covers the entire X- and Ku-bands. To aid the design structure, the
88 simulation method was carried out to optimize the geometrical parameters of the proposed MA.

89 In particular, we use the commercial computer simulation technology (CST) Microwave Studio
90 2013 software with a frequency-domain solver to optimize the designed parameters as well as
91 analyze the performance of the proposed MA. In the simulation setup, the periodic boundary
92 conditions are fixed to unit cell for the x and y directions, and the open boundary condition is
93 set in the z -direction. The incident wave (k) is polarized along $-z$ direction. The tetrahedral mesh is
94 applied in the model with an accuracy of 10^{-4} .

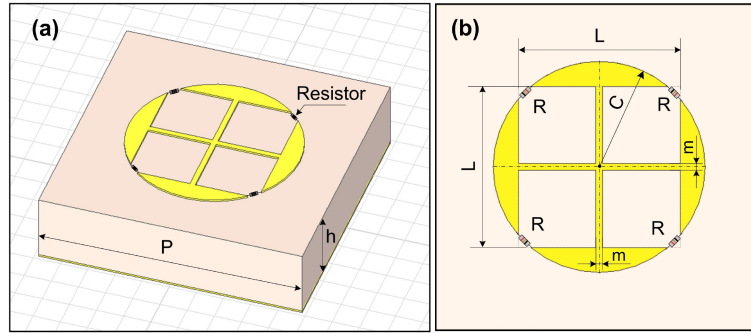


Fig. 1. Schematic of the proposed MA: (a) 3D-view and (b) top view of a unit cell.

TABLE I
Optimized Parameters of the Proposed MA

Parameter	P	h	L	C	m	R
Value	9.7 (mm)	2.5 (mm)	4.8 (mm)	3.15 (mm)	0.2 (mm)	240 (Ω)

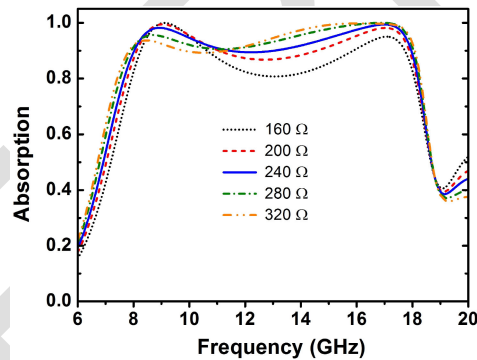


Fig. 2. Absorption spectra of the proposed MA with various values of lumped resistor.

The absorption of the MA can be calculated as equation (1).

$$A(\omega) = 1 - R(\omega) - T(\omega) = 1 - |S_{11}(\omega)|^2 - |S_{21}(\omega)|^2 \quad (1)$$

where, $R(\omega) = |S_{11}(\omega)|^2$ and $T(\omega) = |S_{21}(\omega)|^2$ represent reflection and transmission, respectively. Due to the entire ground plane covers by copper, the transmission becomes zero, thus absorption is simply given by equation (2).

$$A(\omega) = 1 - |S_{11}(\omega)|^2 \quad (2)$$

The MA design aims to work in the frequency range of 8–18 GHz covering the entire X and Ku-bands with an absorption efficiency higher than 90%. To achieve this design goal, we have optimized structural parameters by analyzing the effect of geometrical parameters of h in the range of 1.9–3.1 mm, P in the range of 8.7–10.7 mm, C in the range of 2.75–3.35 mm, L in the range of 2.3–2.6 mm, m in the range of 0.1–0.5 mm, and R in range of 160–320 Ω on the absorption spectra of the proposed MA. Based on the evaluation of simulation results in such a way that absorption spectrum is the widest and its efficiency is the highest, the design parameter optimization of the proposed MA structure is gathered as shown in Table I. With changing the value of lumped resistors in the range from 160 - 320 Ω , the absorption bandwidth is almost unchanged, as shown in Fig. 2. This is due to the resonances is created when the imaginary part of the input admittance

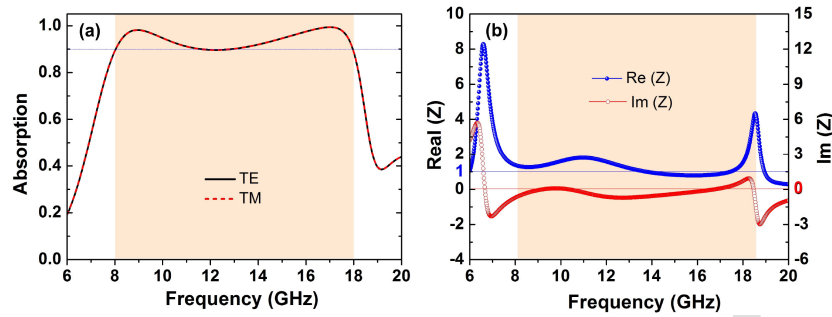


Fig. 3. (a) Absorption spectra and (b) the normalized impedance of the proposed MA under normal incidence.

109 equals zero [43], [44]. The imaginary part of the input admittance depends only on the inductor
 110 and capacitor parameters determined by the shape of metallic resonator of the unit cell but not
 111 on lumped resistor (R). However, the R parameter determines the input impedance of MA, thus
 112 leading to the change in the absorptivity of the proposed MA as seen in Fig. 2. The absorptivity is
 113 above 90% in the desired frequency band ranging from 8 - 18 GHz when R varies from 240 to 280
 114 Ω . Therefore, in this design, the R is chosen at 240 Ω to obtain strong resonant peaks.

115 III. Results and Discussion

116 Fig. 3(a) shows the absorption spectra of the proposed MA for both TE and TM polarizations.
 117 The absorption spectra of the proposed MA for TE and TM polarizations are superimposed to
 118 each other. It possesses the absorption response with absorptivity above 90% in a wide frequency
 119 band from 8 - 18 GHz covering the entire X- and Ku-bands. Furthermore, two distinct absorption
 120 peaks are found at 8.9 GHz and 17.1 GHz, with corresponding absorptivities of 98.2% and 99.4%,
 121 respectively. The relative bandwidth is used to evaluate the absorption performance of the MA,
 122 which is calculated as equation (3), where f_U and f_L are the highest and lowest frequency of
 123 absorption band with absorptivity higher than 90%. It proves the relative bandwidth (RBW) of the
 124 proposed MA can reach to 76.92%, indicating that the designed MA achieves the ultra-broadband
 125 absorption properties.

$$RBW = 2 \times \frac{f_U - f_L}{f_U + f_L} \quad (3)$$

126 The absorption mechanism of the proposed MA can be explained by the impedance matching
 127 between the MA structure and the free space. The normalized impedance of the MA is given by
 128 equation (4) [45], [46].

$$Z = \sqrt{\frac{(1 + S_{11})^2 - S_{21}^2}{(1 - S_{11})^2 - S_{21}^2}} = \frac{1 + S_{11}}{1 - S_{11}}. \quad (4)$$

129 Due to its impedance matching, a smaller amount of power is reflected from the structure thus
 130 maximum absorptivity occurs at the desired frequency band. Fig. 3(b) shows the normalized
 131 impedance of the proposed MA. It is seen that real and imaginary part are nearly unity and
 132 zero over a wide frequency range from 8 to 18 GHz which confirms the presence of broadband
 133 absorption.

134 To further investigate the physical mechanism, we have simulated the electric field and surface
 135 current distributions of the proposed MA at the resonant frequencies of 8.9 GHz and 17.1 GHz in
 136 the XOY plane, as presented in Fig. 4. As seen in Figs. 4(a) and (d), the electric field is concentrated
 137 at a particular part of MA corresponding to a specific frequency. At the lower resonant frequency

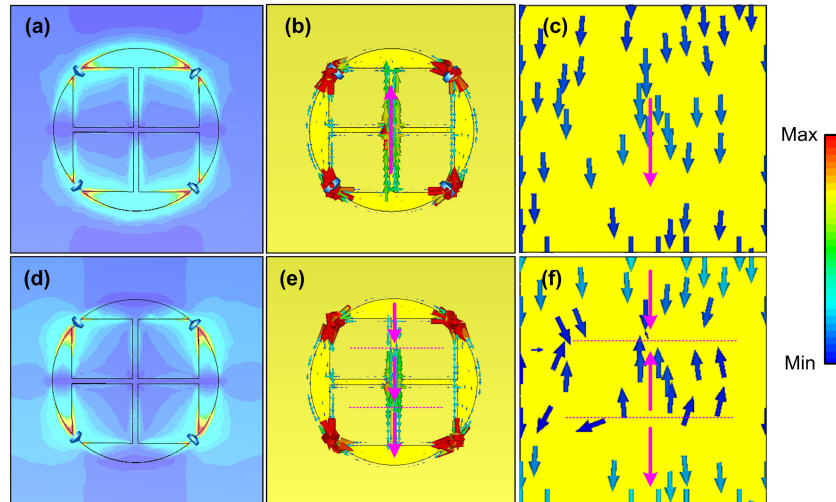


Fig. 4. (a),(d) the electric field distribution and surface current distributions on (b),(e) the top layer and (c),(f) the bottom layer of the proposed absorber at the resonant frequencies of 8.9 GHz and 17.1 GHz, respectively.

of 8.9 GHz, the electric field harvests at the gaps and the vertical shape of the metallic resonator. Meanwhile, at the resonant frequency of 17.1 GHz, the electric field accumulates at the gaps and the horizontal shape of the metallic resonator. The surface current distributions on the top and bottom metallic layer of the proposed MA at 8.9 GHz and 17.1 GHz are presented in Figs. 4(b),(c) and (e),(f), respectively. It is clear from Figs. 4(b) and (c), at the lower frequencies of 8.9 GHz, the top surface current is anti-parallel with the bottom surface current, indicating that the magnetic resonance is contributed to the resonant frequency. At the higher resonant frequency of 17.1 GHz, the bottom surface current is divided to three regions, where the currents on adjacent regions are anti-parallel, as shown in Fig. 4(f). Meanwhile, the top surface current is kept in the same direction in the three regions as seen in Fig. 4(e). This interesting effect is caused by the same order of the periodicity and the operational wavelength at 17.1 GHz. Therefore, the periodic metallic patterns of proposed MA can be regarded as a two-dimensional metallic grating, which creates the guided-mode resonances (GMRs) [47]–[51]. It was reported that the magnetic resonance excited in MA structure that obtained the wide-angle insensitivity for both TE and TM polarizations [52], [53]. It is due to the forming of the induced magnetic field inside the MA structure that can efficient trap the incident magnetic field for wide-incident angle. Furthermore, the efficient and wide-angle broadband absorption response is attributed to the existing of the GMR resonances in the meta-surface structure [54]. Therefore, wide-angle insensitive wideband absorption response in the proposed design loaded lumped resistors is due to the synergy of magnetic and the GMR resonances.

For practical applications, the design MA can maintain the broadband absorption response with a wide incident angle that is a main important factor because the electromagnetic (EM) wave is obliquely incident onto the surface. Thus, the simulated dependence of the absorptivity on the frequency and the incident angles in the range of 0–50° for both TE and TM polarizations is implemented, as depicted in Fig. 5. It can be seen that for both polarizations, the absorptivity of the proposed MA decreases with increasing the incident angle. However, the proposed absorber can maintain the high absorption intensity above 70 % with increasing the incident angle up to 50° for both TE and TM polarizations. Moreover, the absorptivity can keep as high as 80% in the whole operating frequency range from 8 GHz to 12 GHz, when incident angle changes from 0° to 35° for TE polarization and 0° to 40° for TE polarization. It indicates that the proposed MA has a good broadband absorption performance for a wide incident angle.

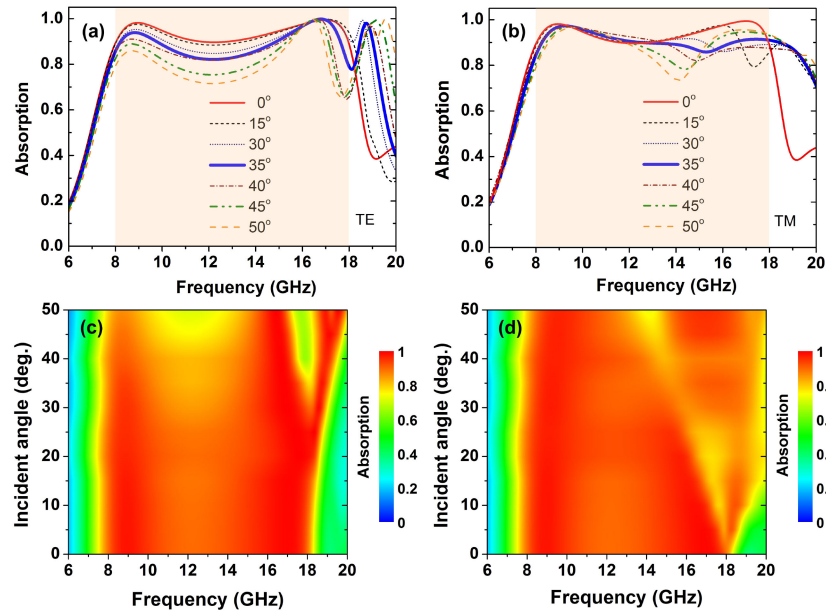


Fig. 5. Absorption spectra and the corresponding absorption maps of the proposed MA with different incident angles for (a),(c) TE and (b),(d) TM polarizations, respectively.

169 We also investigate the effect of the polarization angle on the performance of the proposed MA
 170 for both TE and TM polarizations. It can be seen in Fig. 6, for both polarizations, the absorptivity
 171 is not changed in the whole operation frequency band (8-18 GHz) with varying of the polarization
 172 angle from 0 to 90°. It proves that the proposed MA is polarization insensitivity due to its symmetry
 173 structure.

174 To verify the performance of the designed MA, device fabrication was using the conventional
 175 photolithography process. The structural parameters of the fabrication sample are fixed the same
 176 as the simulated model. The material used in the device fabrication is the copper coated FR-4
 177 substrate on both sides with a copper thickness of 0.035 mm, FR-4 substrate thickness of 2.5 mm,
 178 and a relative dielectric constant of 4.3. The surface mount resistors with size 0402 and resistance
 179 of 240 Ω with 1% tolerance are chosen as lumped resistors. The fabricated sample image is
 180 illustrated in Fig. 7, which contains 20 \times 20 unit cells and 1600 resistors and has an oversize
 181 of 194 mm \times 194 mm. To analyze the absorption performance of fabricated MA, the reflection
 182 coefficients as a function of frequency were measured by the Rohde and Schwarz ZNB20 vector
 183 network analyzer together with two identical linearly polarized standard-gain horn antennas as
 184 transmitter and receiver. The measurement data are collected in the range of 6-18 GHz. Figs. 8
 185 shows the measured absorption spectra of fabricated MA with various oblique angles of 10°, 30°
 186 and 40° for TE and TM polarizations. It can be observed that the experimental results are in good
 187 agreement with the simulation results. The measured absorptivity keeps higher than 0.8 in the
 188 range of 8-18 GHz with incident angle up to 40° for both TE and TM polarizations. It confirms that
 189 the designed MA is a wide incident angle insensitivity.

190 Finally, we have compared the performance of the proposed MA with other recently reported
 191 broadband MAs designed based on lumped resistors. Table II shows the MA properties in terms of
 192 operating frequency, the periodicity of unit-cell and thickness with respect to the lowest absorption
 193 frequency, relative bandwidth, and unit-cell characteristics including the number of layers and
 194 lumped resistors. It can be seen from Tab. II, the proposed design has a simple structure with
 195 the smallest thickness and moderate periodicity and excellent performance characterized by the
 196 highest relative bandwidth per layer as well as per lumped resistor, simultaneously.

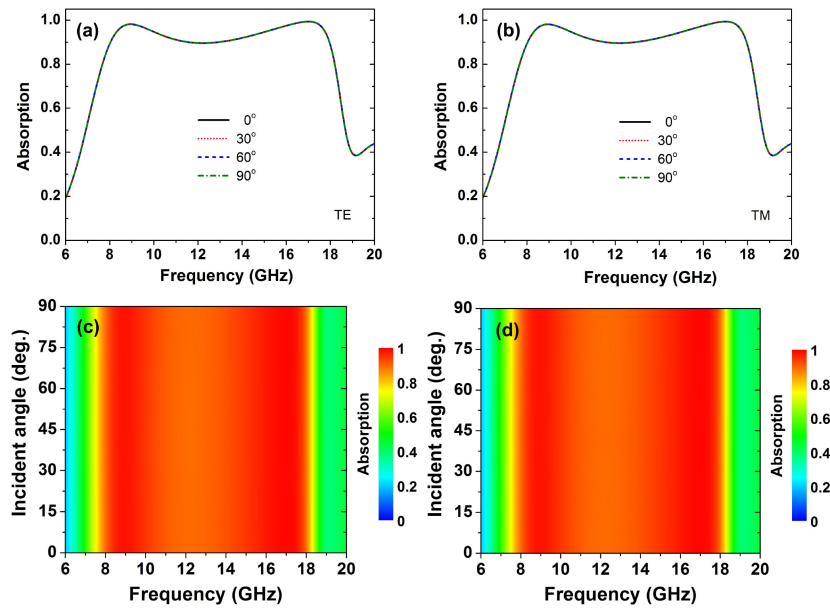


Fig. 6. Absorption spectra and the corresponding absorption maps of the proposed MA with different polarization angles under normal incidence for (a),(d) TE and (b),(d) TM polarizations, respectively.

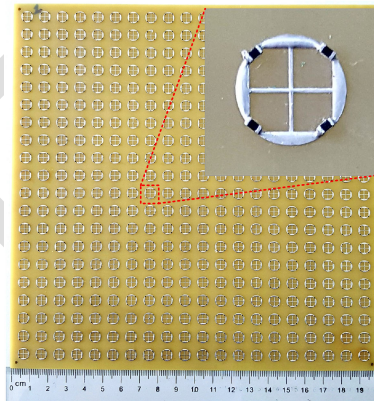


Fig. 7. The image of the fabricated sample and its enlarged view.

TABLE II
Comparison the Performance of the Proposed MA With Other Broadband MAs

Ref.	Working frequency (GHz)	Periodicity of unit-cell (mm)	Thickness (mm)	RBW (%)	Unit-cell characteristics	
					No. layers	No. resistors
[55]	7.2 - 12.5	12.8×12.8 ($0.31\lambda_L$)	5.2 ($0.125\lambda_L$)	53.81	3	6
[56]	5.2 - 18	13×13 ($0.23\lambda_L$)	4.8 ($0.083\lambda_L$)	110.35	3	12
[57]	7.6 - 18.3	10×10 ($0.25\lambda_L$)	3.25 ($0.082\lambda_L$)	82.63	2	4
[58]	3.9 - 10.5	12.5×12.5 ($0.16\lambda_L$)	7.57 ($0.098\lambda_L$)	91.67	2	4
[59]	8.2 - 13.4	15.5×15.5 ($0.42\lambda_L$)	3.0 ($0.082\lambda_L$)	48.15	1	8
[60]	8 - 18	13×13 ($0.36\lambda_L$)	3.175 ($0.085\lambda_L$)	76.92	1	8
[61]	7 - 12.8	14×14 ($0.33\lambda_L$)	3.4 ($0.079\lambda_L$)	58.59	1	4
This work	8 - 18	9.7×9.7 ($0.26\lambda_L$)	2.5 ($0.067\lambda_L$)	76.92	1	4

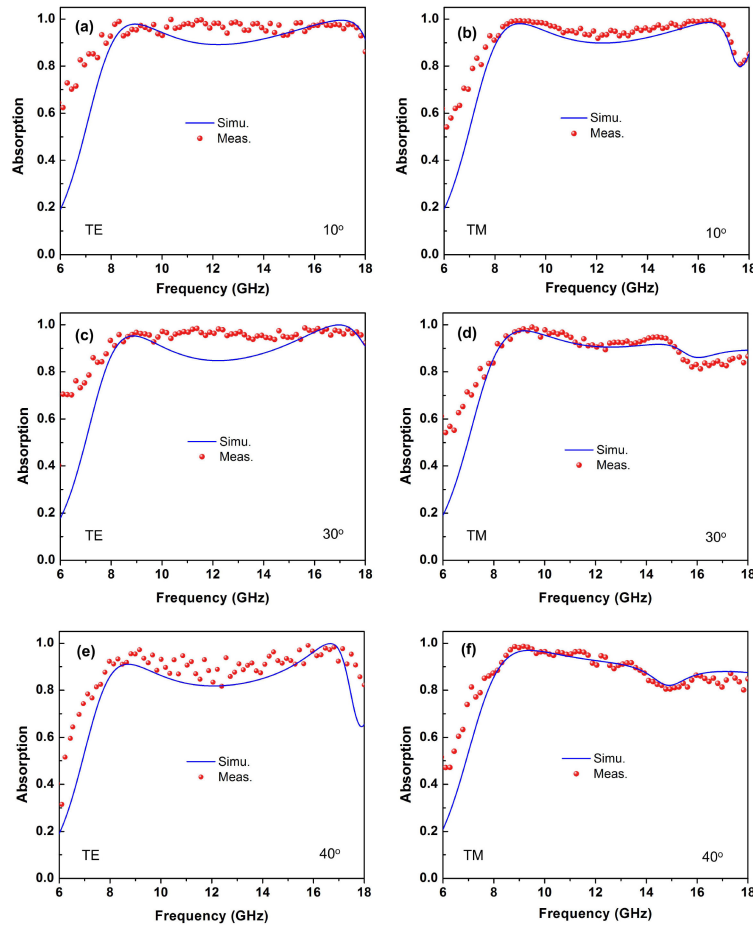


Fig. 8. The measured absorption spectra of the fabricated MA under various incident angles of 10° , 30° , and 40° for (a),(c),(e) TE and (b),(d),(f) TM polarizations, respectively.

197 IV. Conclusion

198 We have proposed a wideband and polarization and wide-angle insensitive MA based on sym-
 199 mmetry structure with surface mount resistors operating in the X- and Ku-bands. The proposed
 200 structure is composed of a periodic array of a top metal symmetry resonator loading with four
 201 lumped resistors, a dielectric substrate of FR-4 backed a continuous metal ground plane. The
 202 absorption performance of the proposed absorber is analyzed by both simulation and experiment.
 203 The experimental result shows that the proposed MA can maintain the absorptivity above 80% in a
 204 frequency range from 8-18 GHz for a wide incident angle up to 40° for both TE and TM polarizations.
 205 Moreover, the proposed MA is insensitive to polarization due to its symmetry structure. The physical
 206 absorption mechanism has been explained by a thorough analysis of the impedance and surface
 207 current distribution. Besides, compared with other absorbers based on lumped resistors, our design
 208 has a simple and compact structure, and excellent performance such as high relative absorption
 209 bandwidth, polarization, and wide-incident insensitivity. Therefore, these suggest that this design is
 210 a promising candidate for X- and Ku-band applications.

211 References

212 [1] J. B. Pendry, "Negative refraction makes a perfect lens," *Phys. Rev. Lett.*, vol. 85, pp. 3966–3969, 2000.

- [2] A. Arbabi, Y. Horie, A. J. Ball, M. Bagheri, and A. Faraon, "Subwavelength-thick lenses with high numerical apertures and large efficiency based on high-contrast transmitarrays," *Nature Commun.*, vol. 6, no. 1, pp. 7069, 2015. 213 Q3
- [3] M. Khorasaninejad and F. Capasso, "Metalenses: Versatile multifunctional photonic components," *Science*, vol. 358, no. 6367, 2017, Art. no. eaam8100. 215
- [4] D. Wen *et al.*, "Helicity multiplexed broadband metasurface holograms," *Nature Commun.*, vol. 6, no. 1, pp. 8241, 2015. 216
- [5] E. Almeida, O. Bitton, and Y. Prior, "Nonlinear metamaterials for holography," *Nature Commun.*, vol. 7, 2016, Art. no. 12533. 217
- [6] J. B. Pendry, D. Schurig, and D. R. Smith, "Controlling electromagnetic fields," *Science*, vol. 312, pp. 1780–1782, 2016. 218
- [7] H. Chen, C. T. Chan, and P. Sheng, "Transformation optics and metamaterials," *Nature Mater.*, vol. 9, pp. 387, 2010. 219
- [8] T. K. T. Nguyen *et al.*, "Simple design of efficient broadband multifunctional polarization converter for x-band applications," *Sci. Rep.*, vol. 11, pp. 2032, 2011. 220
- [9] T. Q. H. Nguyen *et al.*, "Simple design of a wideband and wide-angle reflective linear polarization converter based on crescent-shaped metamaterial for ku-band applications," *Opt. Commun.*, vol. 456, 2021, Art. no. 126773. 221
- [10] N. I. Landy, S. Sajuyigbe, J. J. Mock, D. R. Smith, and W. J. Padilla, "Perfect metamaterial absorber," *Phys. Rev. Lett.*, vol. 100, 2008, Art. no. 207402. 222
- [11] N. Liu, M. Mesch, T. Weiss, M. Hentschel, and H. Giessen, "Infrared perfect absorber and its application as plasmonic sensor," *Nano Lett.*, vol. 10, no. 7, pp. 2342–2348, 2010. 223
- [12] Y. Wang, T. Sun, T. Paudel, Y. Zhang, Z. Ren, and K. Kempa, "Metamaterial-plasmonic absorber structure for high efficiency amorphous silicon solar cells," *Nano Lett.*, vol. 12, no. 1, pp. 440–445, 2012. 224
- [13] P. Rufangura and C. Sabah, "Dual-band perfect metamaterial absorber for solar cell applications," *Vacuum*, vol. 120, pp. 68–74, 2015. 225
- [14] X. Liu, T. Tyler, T. Starr, A. F. Starr, N. M. Jokerst, and W. J. Padilla, "Taming the blackbody with infrared metamaterials as selective thermal emitters," *Phys. Rev. Lett.*, vol. 107, no. 4, 2011, Art. no. 045901. 226
- [15] L. Peng, D. Liu, H. Cheng, S. Zhou, and M. Zu, "A multilayer film based selective thermal emitter for infrared stealth technology," *Adv. Opt. Mater.*, vol. 6, no. 23, 2018, Art. no. 1801006. 227
- [16] A. Kong, B. Cai, P. Shi, and X.-C. Yuan, "Ultra-broadband all-dielectric metamaterial thermal emitter for passive radiative cooling," *Opt. Exp.*, vol. 27, no. 21, pp. 30102–30115, 2019. 228
- [17] X. Liu, J. Gao, L. Xu, X. Cao, Y. Zhao, and S. Li, "A coding diffuse metasurface for RCS reduction," *IEEE Antennas Wireless Propag. Lett.*, vol. 16, pp. 724–727, 2016. 229
- [18] J. Ren, S. Gong, and W. Jiang, "Low-RCS monopolar patch antenna based on a dual-ring metamaterial absorber," *IEEE Antennas Wireless Propag. Lett.* vol. 17, no. 1, pp. 102–105, 2018. 230
- [19] X. Hu *et al.*, "Metamaterial absorber integrated microfluidic terahertz sensors," *Laser Photon. Rev.*, vol. 10, pp. 962–969, 2016. 231
- [20] Y. Wen *et al.*, "Photomechanical meta-molecule array for real-time terahertz imaging," *Microsyst. Nanoeng.*, vol. 3, 2017, Art. no. 17071. 232
- [21] J. Grant, M. Kenney, Y. D. Shah, I. Escorcía-Carranza, and D. R. S. Cumming, "CMOS compatible metamaterial absorbers for hyperspectral medium wave infrared imaging and sensing applications," *Opt. Exp.* vol. 26, no. 8, pp. 10408–10420, 2018. 233
- [22] D. T. Viet *et al.*, "Perfect absorber metamaterials: Peak, multi-peak and broadband absorption," *Opt. Commun.*, vol. 322, no. 1, pp. 209–213, 2014. 234
- [23] W. Ma, Y. Wen, and X. Yu, "Broadband metamaterial absorber at mid-infrared using multiplexed cross resonators," *Opt. Exp.*, vol. 21, no. 25, 2013, Art. no. 30724. 235
- [24] H. Wang and L. Wang, "Perfect selective metamaterial solar absorbers," *Opt. Exp.*, vol. 21, no. 106, 2013, Art. no. A1078. 236
- [25] G. Shen, M. Zhang, Y. Ji, W. Huang, H. Yu, and J. Shi, "Broadband terahertz metamaterial absorber based on simple multi-ring structures," *AIP Adv.*, vol. 8, 2018, Art. no. 075206. 237
- [26] F. Ding, Y. Cui, X. Ge, Y. Jin, and S. He, "Ultra-broadband microwave metamaterial absorber," *Appl. Phys. Lett.*, vol. 100, 2012, Art. no. 103506. 238
- [27] Y. Cui *et al.*, "Ultrabroadband light absorption by a sawtooth anisotropic metamaterial slab," *Nano Lett.*, vol. 12, pp. 1443, 2012. 239
- [28] N. T. Q. Hoa, P. D. Tung, and P. H. Lam, "Wide-angle and polarization-independent broadband microwave metamaterial absorber," *Microw. Opt. Technol. Lett.*, vol. 59, no. 5, pp. 1157–1161, 2017. 240
- [29] N. T. Q. Hoa, P. H. Lam, P. D. Tung, T. S. Tuan, and H. Nguyen, "Numerical study of a wide-angle and polarization-insensitive ultrabroadband metamaterial absorber in visible and near-infrared region," *IEEE Photon. J.*, vol. 11, no. 1, Feb. 2019, Art. no. 4600208. 241
- [30] T. S. Tuan and N. T. Q. Hoa, "Numerical study of an efficient broadband metamaterial absorber in visible light region," *IEEE Photon. J.*, vol. 11, no. 3, Jun. 2019, Art. no. 4600810. 242
- [31] M. Kenney, J. Grant, and D. R. S. Cumming, "Alignment-insensitive bilayer THz metasurface absorbers exceeding 100% bandwidth," *Opt. Exp.*, vol. 27, no. 15, pp. 20886–20900, 2019. 243
- [32] M. Kenney, J. Grant, Y. D. Shah, I. Escorcía-Carranza, M. Humphreys, and D. R. Cumming, "Octave-spanning broadband absorption of terahertz light using metasurface fractal-cross absorbers," *ACS Photon.*, vol. 4, pp. 2604–12, 2017. 244
- [33] P. C. Wu, N. Papisimakis, and D. P. Tsai, "Self-affine graphene metasurfaces for tunable broadband absorption," *Phys. Rev. Appl.*, vol. 6, 2016, Art. no. 044019. 245
- [34] S. Fan and Y. Song, "Bandwidth-enhanced polarization-insensitive metamaterial absorber based on fractal structures," *J. App. Phys.*, vol. 123, no. 8, 2018, Art. no. 085110. 246
- [35] P. Yu *et al.*, "Broadband metamaterial absorbers," *Adv. Optical. Mater.*, vol. 17, 2019, Art. no. 1800995. 247
- [36] S. Li, J. Gao, X. Cao, W. Li, Z. Zhang, and D. Zhang, "Wideband, thin, and polarization-insensitive perfect absorber based the double octagonal rings metamaterials and lumped resistances," *J. App. Phys.*, vol. 116, 2014, Art. no. 043710. 248

- 283 [37] T. Q. H. Nguyen, T. K. T. Nguyen, T. N. Cao, H. Nguyen, and L. G. Bach, "Numerical study of a broadband metamaterial
284 absorber using a single split circle ring and lumped resistors for x-band applications," *AIP Adv.*, vol. 10, 2020,
285 Art. no. 035326.
- 286 [38] Y. Z. Cheng, Y. Wang, Y. Niea, R. Z. Gong, X. Xiong, and X. Wang, "Design, fabrication and measurement of a
287 broadband polarization-insensitive metamaterial absorber based on lumped elements," *J. Appl. Phys.*, vol. 111, 2012,
288 Art. no. 044902.
- 289 [39] D. Lee, H. Jeong, and S. Lim, "Electronically switchable broadband metamaterial absorber," *Sci. Rep.*, vol. 7, p. 4891,
290 2017.
- 291 [40] Y. J. Kim, Y. J. Yoo, J. S. Hwang, and Y. P. Lee, "Ultra-broadband microwave metamaterial absorber based on resistive
292 sheets," *J. Opt.*, vol. 19, 2017, Art. no. 015103.
- 293 [41] K. Chen, X. Luo, G. Ding, J. Zhao, Y. Feng, and T. Jiang, "Broadband microwave metamaterial absorber with lumped
294 resistor loading," *EPJ Appl. Metamaterials*, vol. 6, p. 1, 2019.
- 295 [42] M. Bagmanci, O. Akgol, M. Ozakturk, M. Karaaslan, E. Unal, and M. Bakir, "Polarization independent broadband
296 metamaterial absorber for microwave applications," *Int. J. RF Microw. Comput. Aided Eng.*, vol. 29, no. 1, 2018,
297 Art. no. e21630.
- 298 [43] D. Kundu, A. Mohan, and A. Chakrabarty, "Single-layer wide-band microwave absorber using array of crossed dipoles,"
299 *IEEE Antennas Wireless Propag. Lett.*, vol. 15, pp. 1589–1592, 2016.
- 300 [44] Z. Yao, S. Xiao, Z. Jiang, L. Yan, and B.-Z. Wang, "On the design of ultrawideband circuit analog absorber based on
301 quasi-single-layer FSS," *IEEE Antennas Wireless Propag. Lett.*, vol. 19, no. 4, pp. 591–595, Apr. 2020.
- 302 [45] S. Bhattacharyya and K. V. Srivastava, "Triple band polarization-independent ultra-thin metamaterial absorber using
303 electric field-driven LC resonator," *J. Appl. Phys.*, vol. 115, 2014, Art. no. 064508.
- 304 [46] T. S. Tuan, V. D. Lam, and N. T. Q. Hoa, "Simple design of a copolarization wideband Metamaterial Absorber for C-band
305 applications," *J. Electron. Mater.*, vol. 48, pp. 5018–5027, 2019.
- 306 [47] S. Song, F. Sun, Q. Chen, and Z. Zhang, "Narrow-linewidth and high-transmission terahertz bandpass filtering by
307 metallic gratings," *IEEE Trans. Terahertz Sci. Technol.*, vol. 5, no. 1, pp. 131–136, Jan. 2015.
- 308 [48] Y. Sun, H. Chen, X. Li, and Z. Hong, "Electromagnetically induced transparency in planar metamaterials based on
309 guided mode resonance," *Opt. Commun.*, vol. 392, pp. 142–146, 2017.
- 310 [49] H. Chen, J. Liu, and Z. Hong, "Guided mode resonance with extremely high q-factors in terahertz metamaterials," *Opt.*
311 *Commun.*, vol. 383, pp. 508–512, 2017.
- 312 [50] Z. Yu, H. Che, J. Liu, X. Jing, X. Li, and Z. Hong, "Guided mode resonance in planar metamaterials consisting of two
313 ring resonators with different sizes," *Chin. Phys. B*, vol. 26, 2017, Art. no. 077804.
- 314 [51] D. H. Luu, B. S. Tung, B. X. Khuyen, L. D. Tuyen, and V. D. Lam, "Multi-band absorption induced by near-field coupling
315 and defects in metamaterial," *Optik*, vol. 156, pp. 811–816, 2018.
- 316 [52] T. T. Nguyen and S. Lim, "Wide incidence angle-insensitive metamaterial absorber for both TE and TM polarization
317 using eight-circular-sector," *Sci. Rep.*, vol. 7, pp. 3204, 2017.
- 318 [53] N. T. Q. Hoa, P. D. Tung, N. D. Dung, H. Nguyen, and T. S. Tuan, "Numerical study of a wide incident angle- and
319 polarisation-insensitive microwave metamaterial absorber based on a symmetric flower structure," *AIP Adv.*, vol. 9,
320 2019, Art. no. 065318.
- 321 [54] H. Zhang, M. Luo, Y. Zhou, Y. Ji, and L. Chen, "Ultra-broadband, polarization-independent, wide-angle near-perfect
322 absorber incorporating a one-dimensional meta-surface with refractory materials from UV to the near-infrared region,"
323 *Opt. Mater. Exp.*, vol. 10, pp. 484–491, 2020.
- 324 [55] M. Yoo and S. Lim, "Polarization-independent and ultrawideband metamaterial absorber using a hexagonal artificial
325 impedance surface and a resistor-capacitor layer," *IEEE Trans. Antennas Propag.*, vol. 62, no. 5, pp. 2652–2658,
326 May 2014.
- 327 [56] S. Ghosh, S. Bhattacharyya, and K. V. Srivastava, "Design, characterisation and fabrication of a broadband
328 polarisation-insensitive multilayer circuit analogue absorber," *IET Microw. Antenna Propag.*, vol. 10, no. 8, pp. 850–855,
329 2016.
- 330 [57] H. Chen *et al.*, "Flexible and conformable broadband metamaterial absorber with wide-angle and polarization stability
331 for radar application," *Mater. Res. Exp.*, vol. 5, 2018, Art. no. 015804.
- 332 [58] S. Kalraiya, R. K. Chaudhary, and M. A. Abdalla, "Design and analysis of polarization independent conformal wideband
333 metamaterial absorber using resistor loaded sector shaped resonators," *J. Appl. Phys.*, vol. 125, 2019, Art. no. 134904.
- 334 [59] T. T. Nguyen and S. Lim, "Design of metamaterial absorber using eight-resistive-arm cell for simultaneous broadband
335 and wide-incidence-angle absorption," *Sci. Rep.*, vol. 8, p. 6633, 2018.
- 336 [60] J. Yang and Z. X. Shen, "A thin and broadband absorber using double-square loops," *IEEE Antennas Wireless Propag.*
337 *Lett.*, vol. 6, pp. 388–391, Dec. 2007.
- 338 [61] T. T. Nguyen and S. Lim, "Angle- and polarization-insensitive broadband metamaterial absorber using resistive fan-
339 shaped resonators," *Appl. Phys. Lett.*, vol. 112, 2018, Art. no. 021605.